Research Article

Cédric Bossard*, Henri Granel, Édouard Jallot, Christophe Vial, Hanna Tiainen, Yohann Wittrant, and Jonathan Lao

Polycaprolactone / bioactive glass hybrid scaffolds for bone regeneration

https://doi.org/10.1515/bglass-2018-0010
Received Aug 31, 2018; revised Nov 05, 2018; accepted Nov 10, 2018

Abstract: Bioactive glasses (BG) bond to bone and stimulate bone regeneration, but they are brittle. Inorganic-organic hybrids appear as promising bone substitutes since they associate the bone mineral forming ability of BG with the toughness of polymers. Hybrids comprised of polycaprolactone (PCL) and SiO_2-CaO BG were produced by sol-gel chemistry and processed into porous scaffolds with controlled pore and interconnection sizes. The obtained scaffolds are highly flexible, meaning that PCL effectively introduces toughness. Apatite formation is observed within 24 hours of immersion in simulated body fluid (SBF) and is not limited to the surface as the entire hybrid progressively changes into bone-like minerals. The degradation rate is suitable for bone regeneration with a 13.2% weight loss after 8 weeks of immersion. Primary osteoblasts cultured in scaffolds demonstrate that the samples are not cytotoxic and provide good cell adhesion. The *in vivo* study confirms the bioactivity, biocompatibility and suitable degradation rate of the hybrid. A physiological bone made of trabeculae and bone marrow regenerates. The structure and kinetic of bone regeneration was similar to the implanted commercial standard based on bovine bone, demonstrating that this new synthetic PCL-BG hybrid could perform as well as animal-derived bone substitutes.

Keywords: Bioactive glass; Polycaprolactone; Hybrid; Scaffold; Synthetic bone substitute

1 Introduction

BG are a class of bone substitutes first developed by Hench in 1969 [1]. They have been the focus of much research as they strongly bond to bone [2], they resorb as bone regenerates and their dissolution products stimulate osteoblasts at the genetic level [3]. These unique properties have led to the commercialization of BG, first in the form of monoliths (MEP®, 1985) and later in the form of particulates (PerioGlas®, 1993). However, BG have not been commercialized under a spongy bone-like structure yet. Cancellous bone has a 3-dimensional porous structure that allows cell invasion and fluid flow, thus promoting angiogenesis and osteogenesis [4, 5]. Although BG scaffolds mimicking bone have been successfully fabricated, their high porosity combined with the brittle nature of BG prevents them from being viable in cyclic load-bearing applications [6]. In order to improve the mechanical properties of scaffolds, BG particles can be dispersed in a bioresorbable polymer which introduces toughness to the material. The main drawback of these composites is that the organic and inorganic phases degrade at different rates, thereby causing mechanical instability and release of BG particles *in vivo* [7]. In BG-polymer hybrids, the interpenetration of the two phases at a molecular level provides more uniform and stable properties [7]. Another key advantage of hybrid sol-gel materials is the potential for tailoring their degradation rates and their mechanical properties through a controlled covalent linkage between the organic and inorganic chains [8].

While BG-based hybrid scaffolds have become of increasing interest in the field of biomaterials, their complex synthesis constitutes a chemical challenge that hinders their development. Indeed, the presence of a poly-

***Corresponding Author: Cédric Bossard:** Université Clermont Auvergne, CNRS/IN2P3, Laboratoire de Physique de Clermont, BP 10448, F-63000 Clermont-Ferrand, France;
Email: cedric.bossard@clermont.in2p3.fr
Henri Granel, Yohann Wittrant: Université Clermont Auvergne, INRA, UNH, Unité de Nutrition Humaine, CRNH Auvergne, F-63000 Clermont-Ferrand, France
Édouard Jallot, Jonathan Lao: Université Clermont Auvergne, CNRS/IN2P3, Laboratoire de Physique de Clermont, BP 10448, F-63000 Clermont-Ferrand, France
Christophe Vial: Université Clermont Auvergne, CNRS, Sigma Clermont, Institut Pascal, F-63000, Clermont-Ferrand, France
Hanna Tiainen: Department of Biomaterials, Institute of Clinical Dentistry, University of Oslo, Geitmyrsveien 69-71, 0455 Oslo, Norway

mer at an early stage of the sol-gel process forbids thermal treatments, which are commonly employed to incorporate calcium ions into the BG silicate network. Calcium is essential for the bioactivity of BG and it is known to trigger osteoblast proliferation and differentiation [9]. When synthesizing hybrid materials, calcium alkoxides precursors are preferred to salts, like $CaCl_2$ and $Ca(NO_3)_2$, as they allow effective calcium incorporation even at low temperatures [10]. Nevertheless, their high sensitivity to water can lead to premature gelation of the BG sol and make it more challenging to produce a macroporous structure [11, 12]. Therefore, although many hybrid scaffolds have been created in the recent years, they either do not contain calcium and possess a limited bioactivity [13–15], or they do not incorporate calcium due to the use of salts [15–17]. Only a few BG-based hybrids with well incorporated calcium were obtained, but they were in the form of dense [12, 18] or fibre [11] materials. To avoid the restrictions that arise from the use of calcium, borophosphosilicate glasses SiO_2-B_2O_3-P_2O_5 are a possible alternative as boron is known to accelerate the degradation of BG and induce a faster apatite precipitation on its surface [19]. This means that, even though borophosphosilicate glasses do not contain calcium, they have the potential to be bioactive [20].

In a previous work, we developed a protocol to fabricate BG-gelatin hybrid scaffolds with controlled and tuneable porosity and we showed that the calcium was successfully incorporated at room temperature [21]. Initially, the materials degraded rapidly in SBF, which was attributed to the weak interactions (hydrogen bonds and van der Waals interactions) between the organic and inorganic phases. But when a coupling agent was employed, the gelatin chains cross-linked to the silicate network and the degradation was significantly slowed down. Likewise, several authors report the fast degradation of hybrids even with the use of a coupling agent. For example, Poologasundarampillai *et al*. mention a release of 60% of γ-polyglutamic acid within 2 weeks of soaking in SBF [12], and Li *et al*. mention a 43% weight loss of BG-polyethylene glycol monoliths after 3 weeks [18]. An optimal bone substitute should act as a temporary template and degrade at a specific rate; ideally, it should degrade at the same rate as bone grows, so that mechanical properties are maintained. As yet, most of the BG-based hybrids presented in the literature do not meet this requirement.

In the present study, we adapted the aforesaid protocol to fabricate BG-PCL hybrid scaffolds. FDA-approved PCL is a bioresorbable aliphatic polyester that has been suggested for a wide range of applications such as drug delivery systems, medical devices and tissue engineering [22]. It has a slow degradation rate compared to other polymers (up to 4 years) [23], making it more suitable for long-term degradation applications like bone graft. The apatite-forming ability, degradation rate, mechanical properties, cytotoxicity and *in vivo* performance of the obtained BG-PCL hybrid scaffolds were investigated.

2 Materials and methods

2.1 Synthesis of a hybrid solution

A BG oligomer solution was obtained using tetraethyl orthosilicate (TEOS) (99% purity, Aldrich) and calcium ethoxide (Gelest). TEOS was first hydrolysed in ethanol (absolute, Aldrich) by adding 2 M HCl (obtained from 37% fuming, Aldrich) (molar ratio ethanol : H_2O : TEOS : HCl = 3.7 : 2 : 1 : 0.07). The same volume of ethanol was used for the dilution of calcium ethoxide and the two solutions were mixed together to obtain a sol which was left for condensation. In parallel, PCL (M_n = 80,000 g·mol^{-1}, Aldrich) was dissolved in an appropriate solvent and then mixed with the inorganic sol for 2 hours for homogenisation and further condensation.

2.2 Fabrication of scaffolds

Scaffolds were obtained using a porogen leaching method. Paraffin microspheres were fabricated by emulsifying paraffin in hot water as described by Ma *et al*. [24]. After sieving, the 400–600 µm spheres were stacked in polyethylene moulds and heated at 40°C to partially fuse them. The BG-PCL hybrid solution was then poured onto the stack of microspheres and centrifuged at 6,000 rpm for a complete infiltration. Gelation and ageing of the materials were performed at room temperature for 72 h. The materials were immersed in cyclohexane (99.8% purity, Aldrich) for 24 h to dissolve the paraffin porogen. This operation was renewed twice. Finally, the obtained macroporous hybrid scaffolds were rinsed with absolute ethanol to remove the cyclohexane and dried at room temperature. Pore and interconnection sizes were extracted from Scanning Electron Microscopy (SEM) pictures thanks to the ImageJ software.

2.3 Micro-computed tomography

Micro-computed tomography (microCT) was used to determine the three-dimensional microstructure of the scaffolds. The samples were scanned with SkyScan 1172 mi-

croCT imaging system (Bruker microCT, Kontich, Belgium) at 6 µm voxel resolution using source voltage of 40 kV and current of 167 µA without source filter. The samples were rotated 180° around their vertical axis and three absorption images were recorded every 0.4° rotation. The absorption images were then reconstructed with the standard SkyScan reconstruction software (NRecon) to serial coronal-oriented tomograms using 3D cone beam reconstruction algorithm. For the reconstruction, beam hardening was set to 5% and ring artefact reduction to 10. The image analysis of the reconstructed axial bitmap images was performed using the standard SkyScan software (CTan and CTvox) and included thresholding and despeckling (removing objects smaller than 1000 voxels and not connected to the 3D body). In order to eliminate potential edge effects, a rectangular volume of interest (VOI) with a width and length of 5 mm and a height of 3 mm was selected in the centre of the scaffold.

All images underwent 3D analysis, followed by the quantification of interconnectivity *i.e.* the fraction of pore volume in a scaffold that is accessible from the outside through openings of a certain minimum size [25]. A 'shrink-wrap' process was performed between two 3D measurements to shrink the outside boundary of the VOI through any openings with a size equal to or larger than a threshold value (0 - 240 µm were used in this study). Interconnectivity was calculated as follows:

$$\text{Interconnectivity} = (V - V_{shrink-wrap})/(V - V_m),$$

where V is the total volume of VOI, $V_{shrink-wrap}$ is the VOI volume measured after shrink-wrap processing, and V_m is the volume of scaffold material.

2.4 Bioactivity evaluation in SBF

SBF was prepared following Bohner and Lemaitre's recommendations [26]. BG-PCL hybrid scaffolds were immersed in SBF at a ratio of 1 mg·mL^{-1} and put on an orbital shaker with an agitation rate of 250 rpm at 37°C. The scaffolds were glued to the bottom of the flasks to prevent them from floating and placed under vacuum for 5 min to ensure the infiltration of SBF in the pores. After 6 h, 1 day, 3 days and 7 days of interaction, the solutions were filtered with a 0.2 µm paper and the Ca, P and Si concentrations were determined by Inductively Coupled Plasma - Atomic Emission Spectroscopy (ICP-AES). The materials were rinsed with pure ethanol to avoid further mineralization reactions and dried at ambient temperature. SEM imaging was then performed on samples coated with carbon using vacuum sputtering.

Samples were also analysed with PIXE (Particle-Induced X-ray Emission) nuclear microprobe, a technique that is very similar to SEM-EDS or an electron microprobe, but shows increased sensitivity by 100 times. Reacted scaffolds were embedded in Agar resin and cut into slices of about 150 µm thickness with a low speed diamond saw. Quantitative chemical imaging of the obtained cross-sections was carried out at the AIFIRA platform (CENBG, France) using a 3 MeV incident proton beam (beam diameter of 1 µm). An 80 mm^2 Si (Li) detector equipped with a 12 µm-thick beryllium window and an aluminium funny filter (a 100 µm thick filter with a 2 mm hole drilled at its centre, placed in front of the detector window) orientated at 135° with respect to the incident beam axis was used for X-ray detection. Concentrations in Ca, P and Si were determined using the Gupixwin software after calibration against the NIST 620 (soda-lime glass) standard reference material.

2.5 Mechanical testing

Mechanical properties of BG-PCL hybrid scaffolds were assessed using a TA Instruments 2980 Dynamic Mechanical Analyser. Cylindrical scaffolds with a 5 mm height and a 10 mm diameter were compressed at a constant force rate of 1 N·min^{-1} and their deformation was measured over time. The Young's modulus was determined from the slope of the linear elastic regime using the TA Universal Analysis software. The yield strength was determined at the transition from the elastic regime to the stress plateau.

2.6 Degradation study

The degradation of BG-PCL hybrid scaffolds was investigated in SBF. The procedure to follow the mass of the samples over soaking time was similar to the one used for bioactivity testing. After weighing, scaffolds were glued to the bottom of flasks, immersed in SBF at 1 mg·mL^{-1} and placed under vacuum for 5 min. Then, they were put on an orbital shaker with an agitation rate of 250 rpm and at a temperature of 37°C for up to 8 weeks. After interaction, the materials were rinsed with absolute ethanol, dried under vacuum and their mass was measured again.

2.7 Surface wettability

The surface wettability of PCL and BG-PCL hybrid was investigated. Scaffolds were crushed and grains of 100 to 150 µm were compressed into disks of approximately 1 mm in

thickness. 10 μL of distilled water were dropped on the surface of the disks and pictures were taken with an IDS camera. Contact angle between the water and the disk was determined using the ImageJ software.

2.8 *In vitro* cell adhesion and biocompatibility

2.8.1 Cell culture

Primary osteoblast cells were isolated from 3 days old rats according to Declercq *et al.* [27]. Briefly, calvaria were dissected and the cells were extracted through different enzymatic digestions (collagenase IA and dispase II) at 37°C. The cells were then cultivated in Minimum Essential Medium Eagle Alpha Modifications (α-MEM) supplemented with 10% foetal bovine serum and 1% penicillin/streptomycin at 37°C, 5% CO_2 until 80% confluency before being used.

2.8.2 SEM imaging

SEM was performed on primary osteoblasts cultured in scaffolds or on disks. Cells were fixed with a solution of 3% glutaraldehyde in 0.2 mol·L^{-1} sodium cacodylate buffer (pH 7.4) for 1 h and rinsed in cacodylate buffer three times for 10 min each. Afterwards, the samples were dehydrated using a graded ethanol series (70, 95 and 100% ethanol, 10 min for each bath). For SEM examination, the specimens of interest were treated in hexamethyldisilazane (HMDS, Delta Microscopies), dried overnight and coated using a sputter coater equipped with a gold target (Jeol JFC-1300) and observed with a scanning electron microscope (Jeol 6060-LV) at 5 KeV.

2.8.3 Fluorescence microscopy

Fluorescence microscopy was performed on primary osteoblasts cultured 14 days in BG-PCL hybrid scaffolds under orbital agitation. Scaffolds were washed and incubated in fluorescent dye (CyQUANT^{TM} NF Cell Proliferation Assay Kit, Invitrogen) for 30 min. Pictures were taken with inverted fluorescence microscope (AxioObserver Z1).

2.8.4 Cell viability

Scaffolds were first incubated in culture medium for 72 h to avoid the initial burst of calcium ions that may damage cells [28]. Then, primary osteoblasts were seeded in a 96-well plate at a density of 3500 cells per well, and cultured for 96 h in α-MEM medium supplemented with 10% foetal bovine serum in BG-PCL hybrid scaffolds. The cell viability was determined by a XTT method using Viability/Proliferation Kit II (Aldrich) in accordance with supplier recommendations. The optical density was measured through spectrophotometry at 550 nm and compared with the control condition corresponding to the absence of material.

2.9 *In vivo* study

The *in vivo* study was performed at the Centre d'Investigation Clinique–Innovation Technologique (CIC-IT) Bordeaux. All the procedures for rat handling were based on the principles of Laboratory Animal Care formulated by the National Society for Medical Research and approved by the Animal Care and Experiment Committee of University of Bordeaux, France. Experiments were carried out in accredited animal facilities following European recommendations for laboratory animal care. Non-critical size defects in the femoral condyles of 13-week female rats weighing 250 to 300 g were filled with BG-PCL hybrid or commercialized decellularized and deproteinized bovine bone (n = 6 for each material). Bone defects were also left empty as the control condition (sham operation). The animals were anesthetised with isoflurane and a 23 mm^3 defect was created by using a round bur with a diameter of 3.1 mm under copious saline irrigation. The bone cavity was washed with saline solution and filled with the material, then the wound was closed with resorbable inner sutures and cutaneous surgical fastener. The sacrifice was carried out after 9 or 15 weeks by CO_2 asphyxiation. The specimens were immediately fixed in 4% formalin at 4°C for 9 days and then kept in phosphate-buffered saline. Because BG-PCL hybrid is sensitive to temperature, the explants were embedded in the cold-curing resin Technovit® 9100 (Kulzer). The obtained blocks were cut into slices of 7 µm using a RM2255 microtome (Leica) and stained following the Goldner's trichrome method or with von Kossa/MacNeal. Histological sections were eventually observed with a light microscope (Nikon) and analysed using the NIS Elements D software. The different areas (fibrosis, new bone and residual material) were identified and quantified with respect to the surface of the initial

bone defect (histomorphometric analysis). Differences between samples were evaluated with a two-way analysis of variance (ANOVA) followed by a Bonferroni's test. Non-coloured sections were also analysed with a PIXE nuclear microprobe (H^+ 3 MeV).

3 Results and discussion

3.1 Synthesis of a hybrid solution

As mentioned above, calcium alkoxides are required to allow the calcium to enter the silicate network at room temperature. In this work, we opted for calcium ethoxide ($Ca(OEt)_2$) which has already proven to be an adequate calcium source for the synthesis of hybrids.[21] It is worth noting that $Ca(OEt)_2$ was chosen over calcium methoxyethoxide used in pioneer studies [10, 11, 29] because of the safety of the by-products generated (ethanol here, while methanol by-products can be generated in the above references). This is of special importance in the case of incomplete hydrolysis of the alkoxide since the remaining ligands are likely to be released *in vivo*. As $Ca(OEt)_2$ is extremely reactive towards water, a reduced water-to-TEOS molar ratio of 2 was used in our synthesis. This effectively delayed the gelation of the BG sol, which happened after few hours to several days depending on the age of the calcium precursor (hydrolysis reactions take place with atmospheric humidity in the container). Briefly, TEOS is first hydrolysed in an acidified alcoholic solution to form silanol species. Dilute $Ca(OEt)_2$ is then added and condensation reactions occur, resulting in chains of SiO_2-CaO nanoparticles. The amounts of precursors were adjusted to reach a BG composition of 75 wt.% SiO_2– 25 wt.% CaO known to induce rapid bioactivity [30]. Before further condensation leads to gelation, the BG sol is mixed with the polymer solution so that the organic and inorganic chains entangle to create a hybrid containing up to a 40 wt.% BG fraction. Finally, the translucent hybrid solution (Figure 1) can be processed to obtain a macroporous structure.

3.2 Fabrication of scaffolds

In the literature, several techniques have been developed to produce scaffolds from a BG sol, such as the polymer foam reticulation [31] and the sol-gel foaming process [32], but they involve a sintering step and the use of water (respectively) that are not compatible with our hybrid sol – the presence of polymer forbids thermal treatments

Figure 1: A BG-PCL hybrid solution. Its translucency indicates that the organic and inorganic phases are homogeneously mixed.

whereas water provokes a premature gelation. Here we found a convenient way of generating a 3D-interconnected macroporous structure at ambient temperature and without adding water. A porogen leaching method is employed, which results in a highly porous BG-PCL hybrid scaffold as depicted in Figure 2a. The pore size is close to the size of the porogen microspheres, which means that it can be readily controlled through the granulometry of the microspheres (1). Similarly, the interconnection size between pores can be finely tuned by previously heating the stack of microspheres for different times as illustrated in Figure 2b. Indeed, interconnections originate from the contact point between each porogen spheres and their widening can be achieved through partial fusion of the spheres. Both the pore and interconnection sizes are key parameters to vascularisation and cell migration, and while it is generally admitted that the minimal pore size should be 100 µm [33], Karageorgiou and Kaplan reported enhanced bone regeneration and formation of capillaries for pores larger than 200-300 µm and interconnections superior to 50 µm [34]. To follow these recommendations, the scaffolds in the subsequent sections were produced with paraffin spheres ranging from 400 to 600 µm, which gave pores from 300 to 500 µm (Figure 2c), and their prefusion was carried out to reach interconnections between 150 and 200 µm. According to microCT measurements, the scaffolds have relatively thick struts of 145 ± 6 µm and a total porosity of 68.5 ± 1.1% (including barely 0.1% closed porosity). Interconnectivity analysis (2) confirms the well-interconnected structure previously observed by SEM and

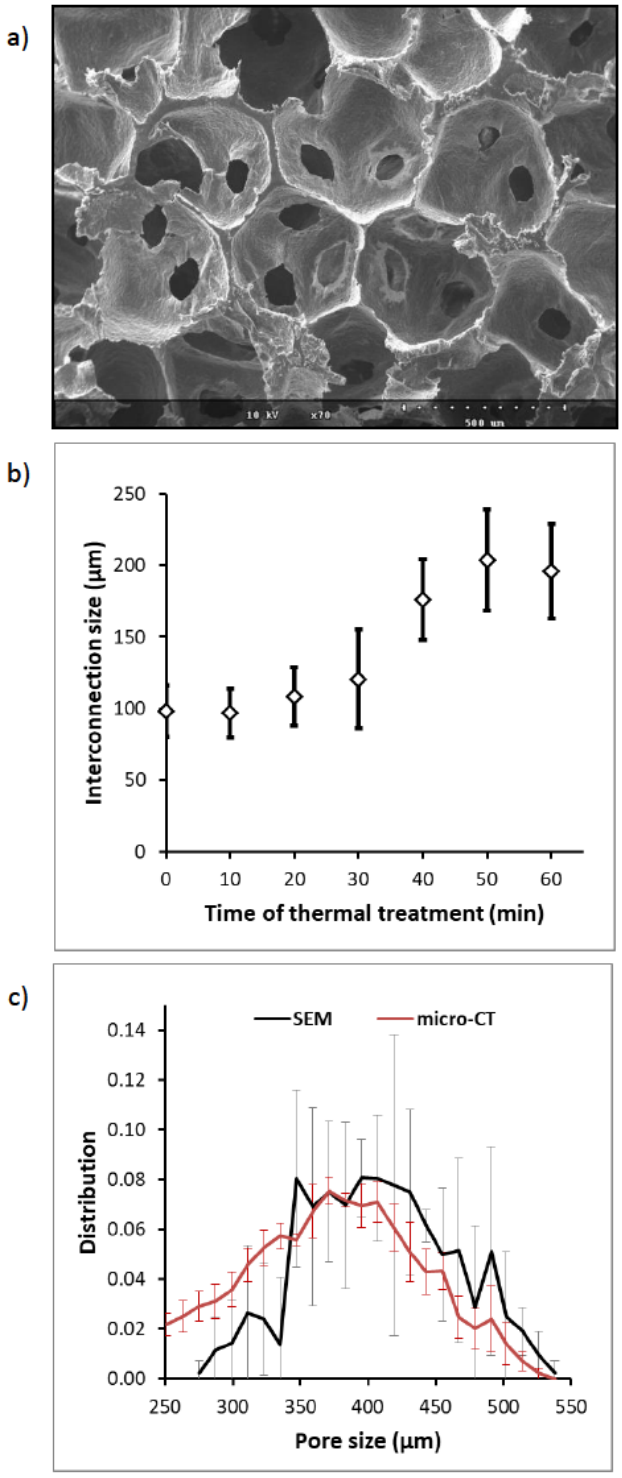

Figure 2: (a) The SEM image of a BG-PCL hybrid scaffold obtained from a stack of microspheres previously heated at 40°C for 60 min. (b) Variation of the mean interconnection size as a function of the time of pre-heating at 40°C. (c) Pore size distribution of scaffolds produced with 400-600 µm porogen spheres according to SEM and microCT measurements.

suggests that the mean interconnection size is around 175-190 µm, which fits SEM measurements.

3.3 Bioactivity evaluation

The bioactivity of BG-PCL hybrids was characterized by immersing scaffolds in SBF for various times. The evolution of Ca, P and Si concentrations as a function of soaking time was followed both in the medium (Figure 3a, ICP-AES) and in the walls of the hybrid scaffolds (Figure 3b, PIXE). The two techniques gave concomitant results that are typical of BG interaction with SBF [35]. At first, Ca and Si ions are released from the samples (Figure 3b, 6h), resulting in an increase of their respective concentrations in SBF (Figure 3a, 6h). These dissolution products, known to stimulate osteoblast proliferation and differentiation [9, 36, 37], trigger the formation of bone mineral by changing the local supersaturation of the medium with regard to apatite precipitation [38]. Here the release of Ca ions is followed by a rapid decrease of Ca and P concentrations in the medium (Figure 3a), which is in accordance with the precipitation of calcium phosphates on the samples (Figure 3b). Moreover, quantitative analysis on the scaffolds immersed for 7 days in SBF shows a Ca/P atomic ratio of 1.6 in the most reacted areas (data not shown) corresponding to that of biological apatites found in bone [39]. SEM on this sample further confirms these observations, as Figure 3c and Figure 3d reveal the formation of an apatite-like layer on its surface.

The cross-sections of scaffolds were also observed by quantitative chemical mapping using the PIXE nuclear microprobe. After 3 days of soaking in SBF (Figure 3e-g), phosphorus is found on the surface as well as in the walls of the hybrid scaffolds. This shows that, unlike conventional BG in which apatite only deposits on the outer layer [40, 41], BG-PCL hybrids have the ability to form apatite throughout the whole volume of the material. This enhanced bioactivity, already observed in BG-gelatin hybrid scaffolds, was previously attributed to the homogeneity of Ca incorporation [21].

3.4 Mechanical properties

Figure 4 illustrates the representative compressive stress-strain curve obtained for BG-PCL hybrid scaffolds. Unlike pure BG scaffolds, brittle crushing of the pore walls does not occur and the samples exhibit a ductile behaviour typical of elastomeric or elastic-plastic cellular solids [42]. The addition of PCL effectively introduces toughness to the

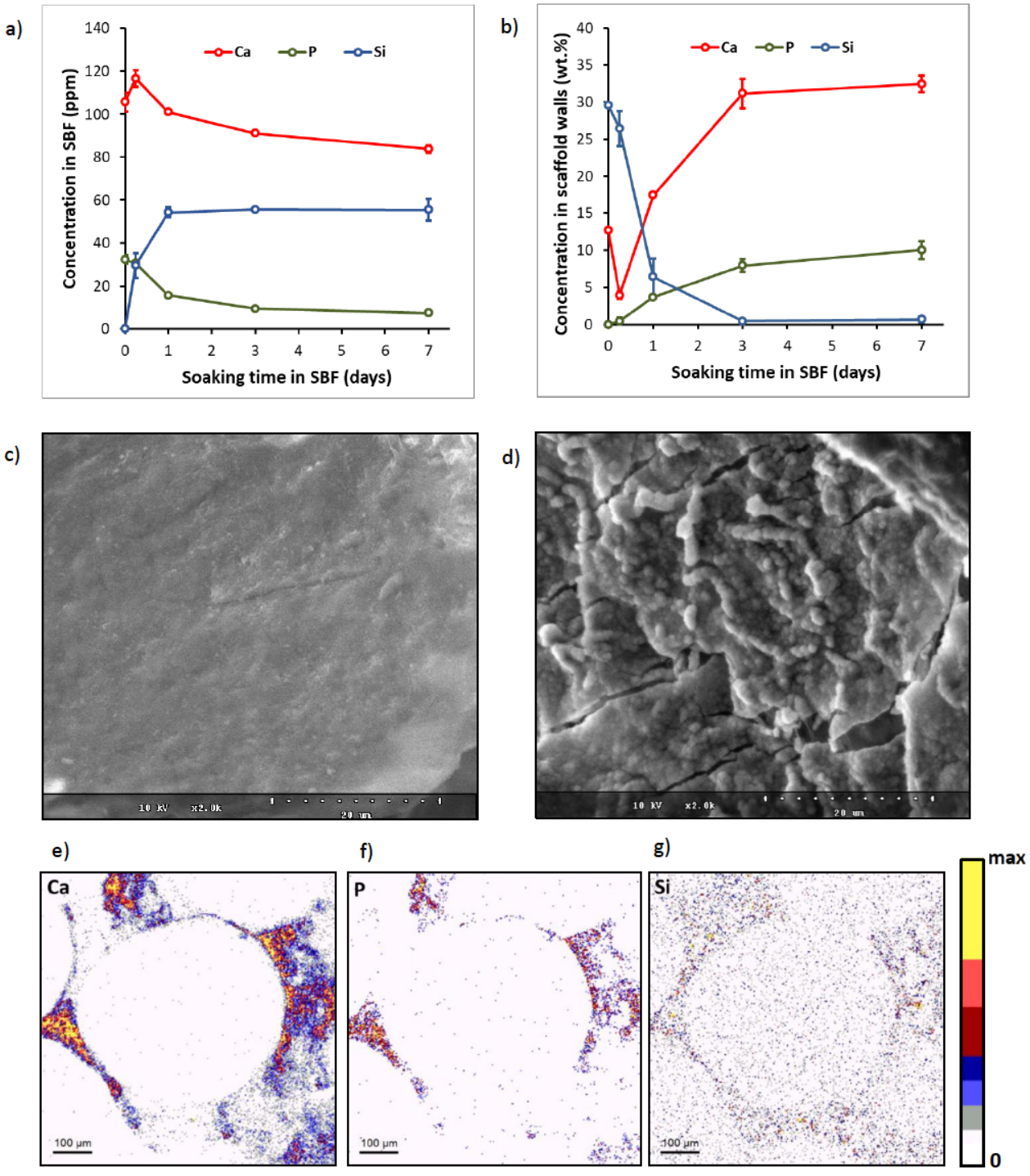

Figure 3: (a) Dissolution products from BG-PCL hybrid scaffolds released in SBF and (b) inorganic composition of BG-PCL hybrid scaffolds as a function of soaking times in SBF. The SEM image of a BG-PCL hybrid scaffold (c) before and (d) after 3 days of soaking in SBF: an apatite-like layer formed on the surface. (e-g) PIXE quantitative chemical imaging of Ca, P and Si inside the cross-section of a BG-PCL hybrid scaffold after 3 days of interaction with SBF.

material and the resultant hybrid can potentially be implanted into sites subjected to cyclic loads. However, the samples display low stiffness as evinced by their elastic modulus of 0.49 MPa (± 0.03 MPa) and yield strength of 0.036 MPa (± 0.003 MPa), which are significantly below those of trabecular bone with the same porosity [42, 43]. Therefore, although BG-PCL hybrid scaffolds may not collapse during handling and during the patient's normal activities thanks to its high flexibility, it is not able to share mechanical load with the host bone. This might not be a major concern since the implant site will progressively recover mechanical properties as new bone grows and bone substitute resorbs. The low stiffness of the scaffolds can be attributed to the polymer used, PCL, which is highly flexible compared to other bioresorbable polymers even at high molecular weight (here, M_n (PCL) = 80000 g.mol^{-1}) [44, 45], and to the lack of bonding between the organic and inorganic phases [46]. As reported in the literature, mechanical properties of PCL-based hybrids can be improved by blending PCL with a stiffer polymer such as polyhydroxybutyrate [15], or through covalent linkage between the PCL chains and the silicate network [47].

3.5 Degradation assay

PCL is known to undergo a two-stage degradation process *in vivo*: first, an uptake of water followed by the hydrolytic chain scission of ester bonds causes a decrease in molecular weight, and second, once the molecular weight has reduced to approximately 3000 g·mol^{-1} the polymer is fully degraded via an intracellular mechanism [22]. Due to the presence of five hydrophobic $-CH_2$ moieties in its repeating units, the de-esterification of PCL is slow and can take longer than 2 years depending on the initial molecular weight of the polymer, whereas intracellular degradation and subsequent excretion last 4 to 5 months [23]. In the present study, the degradation of BG-PCL hybrid scaffolds was investigated *in vitro* by following their mass in SBF for up to 8 weeks (Figure 5a). The samples degrade slowly with only 13.2% weight loss after 8 weeks of soaking in SBF. This degradation rate is more suitable for bone graft applications compared to many hybrids presented in the literature [12, 18]. As evidenced by the bioactivity testing (Figure 3a and Figure 3b), the inorganic phase of BG-PCL hybrids mainly dissolves during the first week of interaction. This implies that the weight losses at 2, 4 and

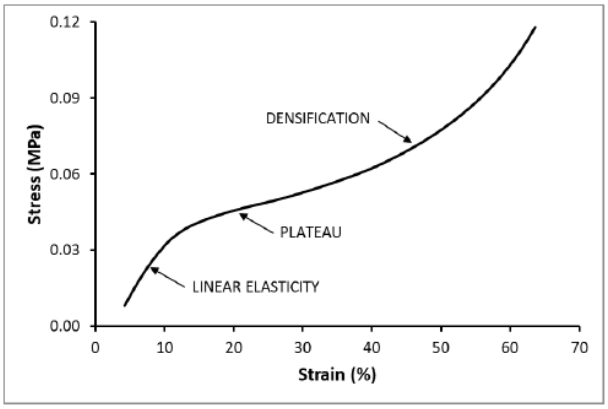

Figure 4: The stress-strain curve of a BG-PCL hybrid scaffold under compression. The sample behaves like an elastomeric or elastic-plastic cellular solid as illustrated by the three regimes: a linear elastic regime corresponding to the cell edge bending, a stress plateau corresponding to the progressive collapse of the macropores, and a final region of densification once the total collapse of the pores throughout the material has occurred.

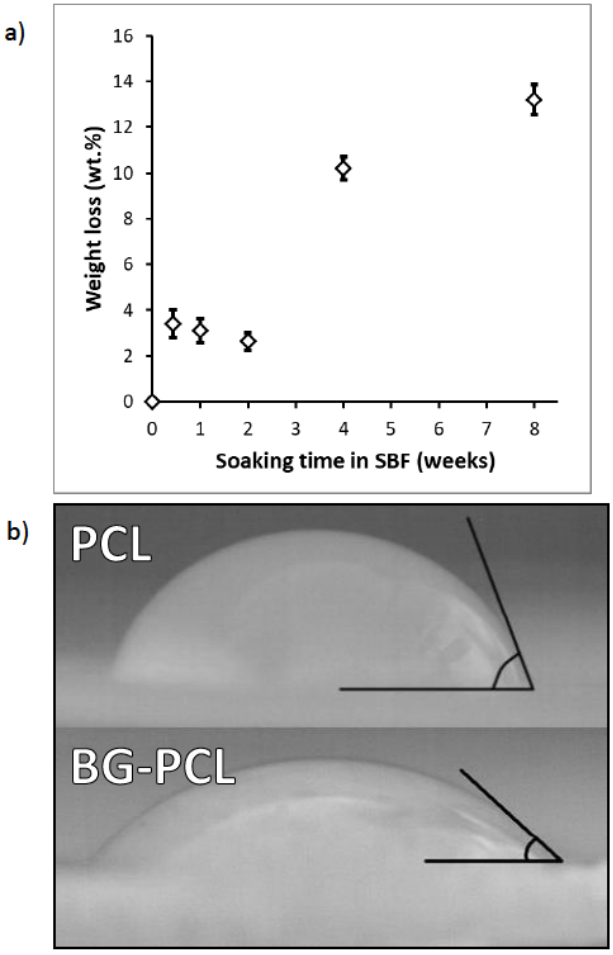

Figure 5: (a) Degradation assay of BG-PCL hybrid scaffolds in SBF. (b) Drops of water on pure PCL and BG-PCL disks for contact angle measurements.

8 weeks are likely to be caused by the degradation of PCL rather than the dissolution of BG. Hence, it appears that de-esterification occurs after few weeks in BG-PCL hybrids instead of months or even years in pure PCL. This substantial difference of kinetics can be explained by the hydrophilicity of BG. Indeed, water contact angle (θ) measurements (Figure 5b) on pure PCL (θ = 83.4° ± 3.1°) and 30 wt.% BG / 70 wt.% PCL hybrid (θ = 56.3° ± 4.8°) disks show that the presence of BG increases the surface wettability of the material. Water absorption, which initiates the hydrolytic chain scission of ester groups, is therefore faster in the hybrid. Moreover, BG is known to induce a local increase in pH while it dissolves. In addition to an antibacterial effect [48], it can be assumed that hydroxide ions catalyse the cleavage of ester linkages.

3.6 *In vitro* cellular behaviour

Cell adhesion on a material surface is a prerequisite to successful cell proliferation and differentiation [49]. Primary osteoblasts were cultured on pure PCL (Figure 6a) and BG-PCL hybrid (Figure 6b) disks. Only few cells adhere to the pure PCL substrate and display a spherical morphology indicative of poor adhesion, whereas cells appear well spread on the hybrid substrate and exhibit a favourable spindle shape with elongated filopodia. Cell adhesion on BG-PCL hybrid can be explained by its increased hydrophilicity described previously (Figure 5b), as more hydrophilic surfaces are highly desirable for osteoblast adhesion [50] and for the regulation of inflammation through the apoptosis of adherent macrophages [51, 52]. Besides, apatite progressively forms throughout the whole material and the obtained bone-like surface may facilitate cell attachment. Indeed, Olmo *et al.* showed that the formation of an apatite layer on 75 wt.% SiO_2 – 25 wt.% CaO BG significantly enhances osteoblast attachment [53].

Primary osteoblasts were also cultured in BG-PCL hybrid scaffolds and the samples were observed by fluorescence microscopy (Figure 6c) and SEM (3). The cells adhere on the walls and are well dispersed inside the scaffold, meaning that BG-PCL hybrid scaffolds allow cell colonisation and cell adhesion.

To determine whether the samples are cytotoxic, primary osteoblasts were cultured in BG-PCL hybrid scaffolds and cell viability was examined after 96 h. Results are presented in Figure 6d and demonstrate that the scaffolds are non-cytotoxic given that no statistical difference is observed with the control conditions.

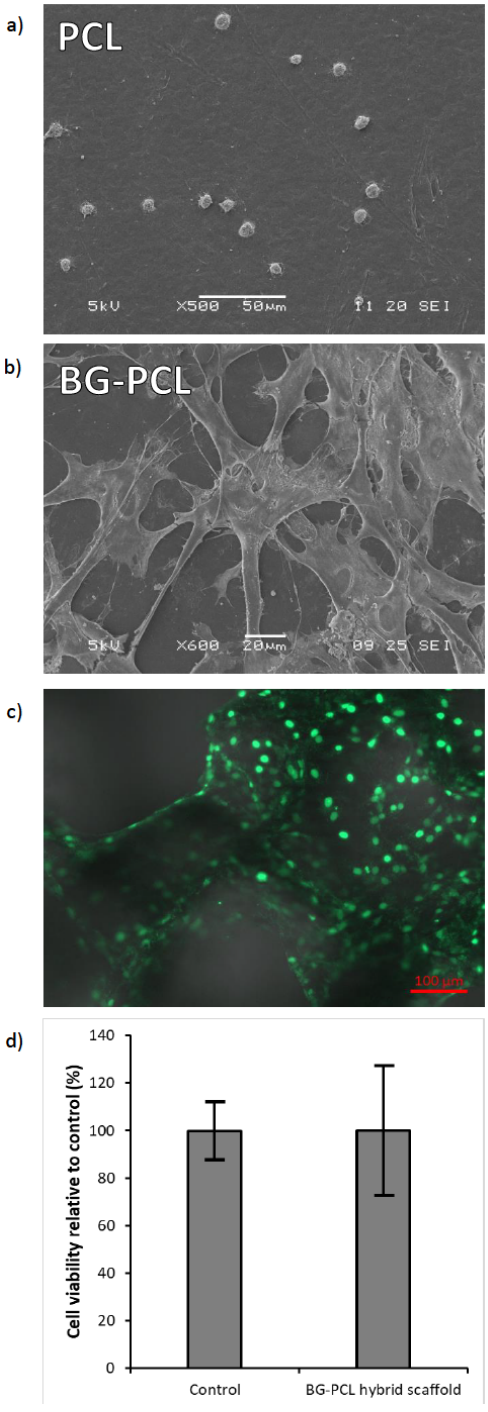

Figure 6: SEM images of primary osteoblasts cultured (a) on pure PCL and (b) BG-PCL hybrid disks. (c) Fluorescence microscopy of primary osteoblasts cultured in a BG-PCL hybrid scaffold. The green dots correspond to cell nuclei. (d) Cytotoxicity evaluation of BG-PCL hybrid scaffolds. Primary osteoblasts were cultured in the presence of a scaffold (or without a scaffold for the control condition). Differences between the sample and the control were estimated using Tukey's HSD post-hoc test (significance level was set to 0.05).

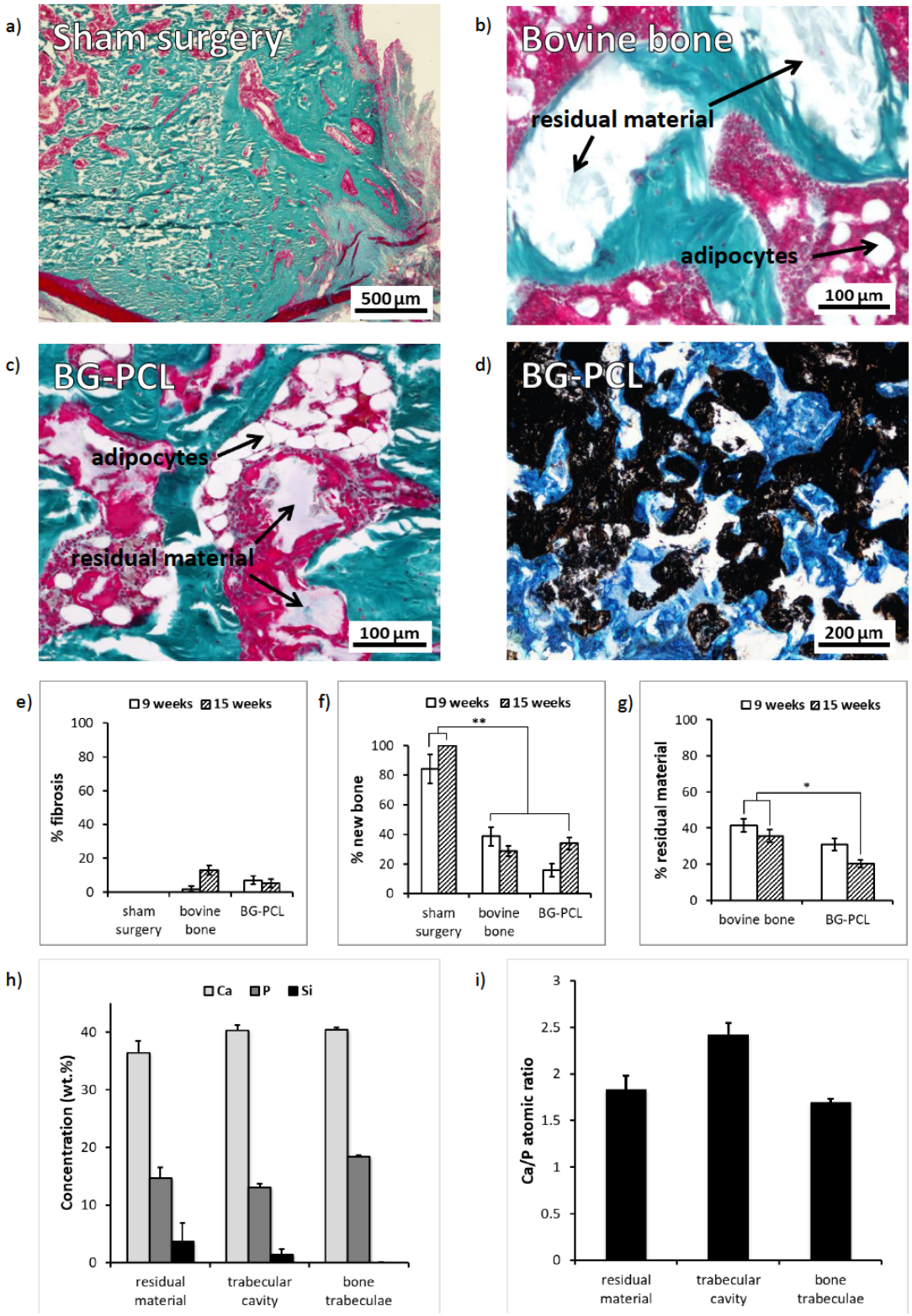

Figure 7: (a-d) Microscope images of histological sections after 15 weeks of implantation strained (a-c) following the Goldner's trichrome method or (d) with von Kossa/MacNeal. (e-g) Estimation of the proportional surfaces occupied by the fibrosis, new bone and residual material as measured by histomorphometry ((*), $P < 0.05$; (**), $P < 0.0001$). (h) Inorganic composition and (i) Ca/P atomic ratio in different areas of the reconstructed bone defect as determined by PIXE.

3.7 *In vivo* study

The *in vivo* performance of BG-PCL hybrids was evaluated in femoral condyles of 13-week rats. Commercialized bovine bone was also implanted as the reference material. Histology was performed after 9 weeks and 15 weeks of implantation (Figure 7a-7g). Bone tissue was identified thanks to the combination of two staining techniques: collagen appears in blue-green when applying the Goldner's trichrome method (Figure 7a-7c) and calcium is stained in black when using von Kossa/MacNeal (Figure 7d). The inflammatory response, known to initiate the regenerative healing process [54], is minimal at 9 weeks and 15 weeks for both materials (Figure 7e). This confirms the biocompatibility of BG-PCL hybrids previously described *in vitro*. As the defect size is not critical, bone entirely regenerates in 15 weeks without the need for a filling material (Figure 7a and Figure 7f), but doing so an undesirable dense structure is obtained for sham-operated rats (non-physiological bone healing). When bovine bone or BG-PCL hybrid is employed, a physiological bone grows as illustrated by the numerous bone trabeculae after 15 weeks of implantation (Figure 7b and Figure 7c). Furthermore, vascularised adipose tissue and bone marrow are found abundantly between the trabeculae, which indicates a well-advanced bone reconstruction for both materials. Quantitative analysis of bone reconstruction (Figure 7f) shows no statistical difference between BG-PCL hybrid and bovine bone. Finally, BG-PCL hybrid appears to be partially degraded after 9 weeks of implantation and even more after 15 weeks: a few of the material is left (Figure 7c), in contrast with bovine bone that barely degraded (Figure 7b). Histomorphometry further confirms these observations, as the bone defect contains significantly less residual material after 15 weeks of implantation when using BG-PCL hybrid instead of bovine bone (Figure 7g).

Histological sections from BG-PCL hybrid samples after 15 weeks of implantation were also analysed with the PIXE nuclear microprobe. Figure 7h shows that the inorganic compositions of the residual material, trabecular cavity and bone trabeculae are similar and resemble that of bone. Only 5 wt.% of Si remains in the hybrid compared to the initial 30 wt.% (Figure 3b), and its low concentration in the trabeculae and trabecular cavity (Figure 7h) suggests that it was removed from the implant site. In fact, Lai *et al.* proved that in rabbits "the silicon eluted from BG in bone tissue was safely excreted through urine with no adverse physiological effects" [55]. The results further reveal the apatite-forming ability and thereby bioactivity of BG-PCL hybrids *in vivo*. Indeed, the residual material is greatly mineralised with an atomic Ca/P ratio close to the one from bone trabeculae (1.8 and 1.7, respectively, Figure 7i). Bioactivity leads to a strong and stable interface between the implant and the host bone and considerably reduces the chance of failure. It is therefore a key advantage of BG-based materials in comparison with other biomaterials like bovine bone or pure PCL.

To conclude this comparative study, the two bone substitutes perform alike in terms of bone healing and biocompatibility; however, BG-PCL hybrid surpasses bovine bone when it comes to degradation and bioactivity.

4 Conclusion

Despite the difficulties that arise from the synthesis of BG-based hybrid scaffolds (integration of calcium ions in the silicate network, fabrication of a macroporous structure with a calcium alkoxide precursor), we were able to fabricate BG-PCL hybrid scaffolds with well incorporated calcium. The scaffold fabrication process is relatively simple and allows the control of both the pore and interconnection sizes. The addition of PCL effectively introduces toughness and the hybrid scaffolds can be implanted into sites subjected to cyclic loads. Even though more work is needed to increase its stiffness to match that of bone, BG-PCL hybrid appears as a promising bone substitute from its overall remarkable properties: shortly after implantation, its enhanced apatite-forming ability observed *in vitro* and *in vivo* may provide a strong interface with host tissues. Because the material contains BG, it has a hydrophilic surface that favours the initial attachment of cells while the release of osteoinductive Si and Ca ions may stimulate the proliferation and differentiation of osteoblasts, thus leading to the regeneration of physiological bone comprised of trabeculae and bone marrow. After few months of implantation, the hybrid still acts as a support for bone growth thanks to its slow degradation *in vivo*. Bone healing (structure and kinetic) is similar when the commercial reference made of bovine bone is employed, with the difference that bovine bone does not degrade.

Acknowledgement: The project was supported by the "Fonds Européens de Développement Régional" (FEDER). The Conseil Régional d'Auvergne is acknowledged for funding. The SATT Grand-Centre is acknowledged for financial support. Dr Mhammed Benbakkar and the Laboratoire Magma et Volcans (UMR 6524, CNRS/Université Blaise Pascal) are acknowledged for ICP-AES measurements. The Centre d'Études Nucléaires de Bordeaux-Gradignan and the AIFIRA staff are acknowledged for

allowing the PIXE experiments. Dr Brigitte Gaillard-Martinie, the Plateau Technique de Microscopie du Centre INRA ARA (UMR 454, MEDIS) and the Centre Imagerie Cellulaire Santé (Faculté de Médecine de Clermont-Ferrand) are acknowledged for SEM imaging on biomaterials with cells. The Centre d'Investigation Clinique–Innovation Technologique (CIC-IT) Bordeaux and Dr Marlène Durand, Samantha Roques, Pr. Sylvain Catros are acknowledged for the *in vivo* implantations and histological investigations.

Conflict of Interests: The authors declare no competing financial interest.

Ethical approval: The research related to animals' use has been complied with all the relevant national regulations and institutional policies for the care and use of animals.

References

[1] Hench, L. L., The story of Bioglass®. J. Mater. Sci.: Mater. Med. 2006, 17 (11), 967-978. DOI: 10.1007/s10856-006-0432-z.

[2] Hench, L. L.; Paschall, H. A., Direct chemical bond of bioactive glass-ceramic materials to bone and muscle. J. Biomed. Mater. Res. 1973, 7 (3), 25-42. DOI: 10.1002/jbm.820070304.

[3] Xynos, I. D.; Edgar, A. J.; Buttery, L. D. K.; Hench, L. L.; Polak, J. M., Gene-expression profiling of human osteoblasts following treatment with the ionic products of Bioglass® 45S5 dissolution. J. Biomed. Mater. Res. 2001, 55 (2), 151-157. DOI: 10.1002/1097-4636(200105)55:2<151::aid-jbm1001>3.0.co;2-d.

[4] McCarthy, I., The physiology of bone blood flow: a review. The Journal of bone and joint surgery. American volume 2006, 88 Suppl 3, 4-9. DOI: 10.2106/jbjs.f.00890.

[5] Ramasamy, S. K.; Kusumbe, A. P.; Schiller, M.; Zeuschner, D.; Bixel, M. G.; Milia, C.; Gamrekelashvili, J.; Limbourg, A.; Medvinsky, A.; Santoro, M. M.; Limbourg, F. P.; Adams, R. H., Blood flow controls bone vascular function and osteogenesis. Nat. Commun. 2016, 7, 13601. DOI: 10.1038/ncomms13601, fhttps://www.nature.com/articles/ncomms13601#supplementary-information.

[6] Fu, Q.; Saiz, E.; Rahaman, M. N.; Tomsia, A. P., Bioactive glass scaffolds for bone tissue engineering: state of the art and future perspectives. Materials Science and Engineering: C 2011, 31 (7), 1245-1256. DOI: http://dx.doi.org/10.1016/j.msec.2011.04.022.

[7] Jones, J. R., Review of bioactive glass: from Hench to hybrids. Acta Biomater. 2013, 9 (1), 4457-4486. DOI: http://dx.doi.org/10.1016/j.actbio.2012.08.023.

[8] Mahony, O.; Tsigkou, O.; Ionescu, C.; Minelli, C.; Ling, L.; Hanly, R.; Smith, M. E.; Stevens, M. M.; Jones, J. R., Silica-gelatin hybrids with tailorable degradation and mechanical properties for tissue regeneration. Adv. Funct. Mater. 2010, 20 (22), 3835-3845. DOI: 10.1002/adfm.201000838.

[9] Maeno, S.; Niki, Y.; Matsumoto, H.; Morioka, H.; Yatabe, T.; Funayama, A.; Toyama, Y.; Taguchi, T.; Tanaka, J., The effect of calcium ion concentration on osteoblast viability, proliferation and differentiation in monolayer and 3D culture. Biomaterials 2005, 26 (23), 4847-4855. DOI: http://dx.doi.org/10.1016/j.biomaterials.2005.01.006.

[10] Yu, B.; Turdean-Ionescu, C. A.; Martin, R. A.; Newport, R. J.; Hanna, J. V.; Smith, M. E.; Jones, J. R., Effect of calcium source on structure and properties of sol-gel derived bioactive glasses. Langmuir 2012, 28 (50), 17465-17476. DOI: 10.1021/la303768b.

[11] Poologasundarampillai, G.; Yu, B.; Jones, J. R.; Kasuga, T., Electrospun silica/PLLA hybrid materials for skeletal regeneration. Soft Matter 2011, 7 (21), 10241-10251. DOI: 10.1039/C1SM06171B.

[12] Poologasundarampillai, G.; Yu, B.; Tsigkou, O.; Wang, D.; Romer, F.; Bhakhri, V.; Giuliani, F.; Stevens, M. M.; McPhail, D. S.; Smith, M. E.; Hanna, J. V.; Jones, J. R., PGA/silica hybrids with calcium incorporated in the silica network by use of a calcium alkoxide precursor. Chemistry (Weinheim an Der Bergstrasse, Germany) 2014, 20 (26), 8149-8160. DOI: 10.1002/chem.201304013.

[13] Mahony, O.; Yue, S.; Turdean-Ionescu, C.; Hanna, J. V.; Smith, M. E.; Lee, P. D.; Jones, J. R., Silica–gelatin hybrids for tissue regeneration: inter-relationships between the process variables. J. Sol-Gel Sci. Technol. 2013, 69 (2), 288-298. DOI: 10.1007/s10971-013-3214-3.

[14] Connell, L. S.; Romer, F.; Suarez, M.; Valliant, E. M.; Zhang, Z.; Lee, P. D.; Smith, M. E.; Hanna, J. V.; Jones, J. R., Chemical characterisation and fabrication of chitosan-silica hybrid scaffolds with 3-glycidoxypropyl trimethoxysilane. J. Mater. Chem. B 2014, 2 (6), 668-680. DOI: 10.1039/c3tb21507e.

[15] Ding, Y.; Roether, J. A.; Boccaccini, A. R.; Schubert, D. W., Fabrication of electrospun poly (3-hydroxybutyrate)/poly (ε-caprolactone)/silica hybrid fibermats with and without calcium addition. Eur. Polym. J. 2014, 55, 222-234. DOI: http://dx.doi.org/10.1016/j.eurpolymj.2014.03.020.

[16] Silva, A. R. P. d.; Macedo, T. L.; Coletta, D. J.; Feldman, S.; Pereira, M. d. M., Synthesis, characterization and cytotoxicity of Chitosan/Polyvinyl Alcohol/Bioactive Glass hybrid scaffolds obtained by lyophilization. Matéria (Rio de Janeiro) 2016, 21, 964-973.

[17] Allo, B. A.; Rizkalla, A. S.; Mequanint, K., Synthesis and electrospinning of polycaprolactone-bioactive glass hybrid biomaterials via a sol-gel process. Langmuir 2010, 26 (23), 18340-18348. DOI: 10.1021/la102845k.

[18] Li, A.; Shen, H.; Ren, H.; Wang, C.; Wu, D.; Martin, R. A.; Qiu, D., Bioactive organic/inorganic hybrids with improved mechanical performance. J. Mater. Chem. B 2015, 3 (7), 1379-1390. DOI: 10.1039/c4tb01776e.

[19] Yao, A.; Wang, D.; Huang, W.; Fu, Q.; Rahaman, M. N.; Day, D. E., In Vitro Bioactive Characteristics of Borate-Based Glasses with Controllable Degradation Behavior. J. Am. Ceram. Soc. 2007, 90 (1), 303-306. DOI: 10.1111/j.1551-2916.2006.01358.x.

[20] Mondal, D.; Rizkalla, A. S.; Mequanint, K., Bioactive borophosphosilicate-polycaprolactone hybrid biomaterials via a non-aqueous sol gel process. RSC Advances 2016, 6 (95), 92824-92832. DOI: 10.1039/C6RA08339K.

[21] Lao, J.; Dieudonne, X.; Fayon, F.; Montouillout, V.; Jallot, E., Bioactive glass-gelatin hybrids: building scaffolds with enhanced calcium incorporation and controlled porosity for bone

regeneration. J. Mater. Chem. B 2016, 4 (14), 2486-2497. DOI: 10.1039/c5tb02345a.
[22] Woodruff, M. A.; Hutmacher, D. W., The return of a forgotten polymer: polycaprolactone in the 21st century. Prog. Polym. Sci. 2010, 35 (10), 1217-1256. DOI: http://dx.doi.org/10.1016/j.progpolymsci.2010.04.002.
[23] Sun, H.; Mei, L.; Song, C.; Cui, X.; Wang, P., The in vivo degradation, absorption and excretion of PCL-based implant. Biomaterials 2006, 27 (9), 1735-1740. DOI: http://dx.doi.org/10.1016/j.biomaterials.2005.09.019.
[24] Ma, Z.; Gao, C.; Gong, Y.; Shen, J., Paraffin spheres as porogen to fabricate poly(L-lactic acid) scaffolds with improved cytocompatibility for cartilage tissue engineering. Journal of Biomedical Materials Research Part B: Applied Biomaterials 2003, 67B (1), 610-617. DOI: 10.1002/jbm.b.10049.
[25] Moore Michael, J.; Jabbari, E.; Ritman Erik, L.; Lu, L.; Currier Bradford, L.; Windebank Anthony, J.; Yaszemski Michael, J., Quantitative analysis of interconnectivity of porous biodegradable scaffolds with micro-computed tomography. Journal of Biomedical Materials Research Part A 2004, 71A (2), 258-267. DOI: 10.1002/jbm.a.30138.
[26] Bohner, M.; Lemaitre, J., Can bioactivity be tested in vitro with SBF solution? Biomaterials 2009, 30 (12), 2175-2179. DOI: http://dx.doi.org/10.1016/j.biomaterials.2009.01.008.
[27] Declercq, H.; Van den Vreken, N.; De Maeyer, E.; Verbeeck, R.; Schacht, E.; De Ridder, L.; Cornelissen, M., Isolation, proliferation and differentiation of osteoblastic cells to study cell/biomaterial interactions: comparison of different isolation techniques and source. Biomaterials 2004, 25 (5), 757-768. DOI: https://doi.org/10.1016/S0142-9612(03)00580-5.
[28] Midha, S.; Kim, T. B.; van den Bergh, W.; Lee, P. D.; Jones, J. R.; Mitchell, C. A., Preconditioned 70S30C bioactive glass foams promote osteogenesis in vivo. Acta Biomater. 2013, 9 (11), 9169-9182. DOI: http://dx.doi.org/10.1016/j.actbio.2013.07.014.
[29] Pereira, M. M.; Clark, A. E.; Hench, L. L., Calcium phosphate formation on sol-gel-derived bioactive glasses in vitro. J. Biomed. Mater. Res. 1994, 28 (6), 693-698. DOI: 10.1002/jbm.820280606.
[30] Isaac, J.; Nohra, J.; Lao, J.; Jallot, E.; Nedelec, J.-M.; Berdal, A.; Sautier, J.-M., Effects of strontium-doped bioactive glass on the differentiation of cultured osteogenic cells. eCells and Materials Journal 2011, 21, 130-143.
[31] Wang, X.; Li, X.; Ito, A.; Sogo, Y., Synthesis and characterization of hierarchically macroporous and mesoporous CaO–MO–SiO2–P2O5 (M=Mg, Zn, Sr) bioactive glass scaffolds. Acta Biomater. 2011, 7 (10), 3638-3644. DOI: http://dx.doi.org/10.1016/j.actbio.2011.06.029.
[32] Sepulveda, P.; Jones, J. R.; Hench, L. L., Bioactive sol-gel foams for tissue repair. J. Biomed. Mater. Res. 2002, 59 (2), 340-348. DOI: 10.1002/jbm.1250.
[33] Hulbert, S. F.; Morrison, S. J.; Klawitter, J. J., Tissue reaction to three ceramics of porous and non-porous structures. J. Biomed. Mater. Res. 1972, 6 (5), 347-374. DOI: 10.1002/jbm.820060505.
[34] Karageorgiou, V.; Kaplan, D., Porosity of 3D biomaterial scaffolds and osteogenesis. Biomaterials 2005, 26 (27), 5474-5491. DOI: http://dx.doi.org/10.1016/j.biomaterials.2005.02.002.
[35] Ohtsuki, C.; Kokubo, T.; Yamamuro, T., Mechanism of apatite formation on CaO-SiO2-P2O5 glasses in a simulated body fluid. J. Non-Cryst. Solids 1992, 143, 84-92. DOI: http://dx.doi.org/10.1016/S0022-3093(05)80556-3.
[36] Kim, E.-J.; Bu, S.-Y.; Sung, M.-K.; Choi, M.-K., Effects of silicon on osteoblast activity and bone mineralization of MC3T3-E1 cells. Biol. Trace Elem. Res. 2013, 152 (1), 105-112. DOI: 10.1007/s12011-012-9593-4.
[37] Zou, S.; Ireland, D.; Brooks, R. A.; Rushton, N.; Best, S., The effects of silicate ions on human osteoblast adhesion, proliferation, and differentiation. Journal of Biomedical Materials Research Part B: Applied Biomaterials 2009, 90B (1), 123-130. DOI: 10.1002/jbm.b.31262.
[38] Lu, X.; Leng, Y., Theoretical analysis of calcium phosphate precipitation in simulated body fluid. Biomaterials 2005, 26 (10), 1097-1108. DOI: http://dx.doi.org/10.1016/j.biomaterials.2004.05.034.
[39] Dorozhkin, S. V.; Epple, M., Biological and medical significance of calcium phosphates. Angewandte Chemie International Edition 2002, 41 (17), 3130-3146. DOI: 10.1002/1521-3773(20020902)41:17<3130::AID-ANIE3130>3.0.CO;2-1.
[40] Kokubo, T., Apatite formation on surfaces of ceramics, metals and polymers in body environment. Acta Mater. 1998, 46 (7), 2519-2527. DOI: http://dx.doi.org/10.1016/S1359-6454(98)80036-0.
[41] Vallet-Regí, M.; Ragel, C. V.; Salinas, Antonio J., Glasses with medical applications. Eur. J. Inorg. Chem. 2003, 2003 (6), 1029-1042. DOI: 10.1002/ejic.200390134.
[42] Gibson, L. J., Biomechanics of cellular solids. J. Biomech. 2005, 38 (3), 377-399. DOI: http://dx.doi.org/10.1016/j.jbiomech.2004.09.027.
[43] Kopperdahl, D. L.; Keaveny, T. M., Yield strain behavior of trabecular bone. J. Biomech. 1998, 31 (7), 601-608. DOI: http://dx.doi.org/10.1016/S0021-9290(98)00057-8.
[44] Engelberg, I.; Kohn, J., Physico-mechanical properties of degradable polymers used in medical applications: a comparative study. Biomaterials 1991, 12 (3), 292-304. DOI: http://dx.doi.org/10.1016/0142-9612(91)90037-B.
[45] Van de Velde, K.; Kiekens, P., Biopolymers: overview of several properties and consequences on their applications. Polym. Test. 2002, 21 (4), 433-442. DOI: http://dx.doi.org/10.1016/S0142-9418(01)00107-6.
[46] Rezwan, K.; Chen, Q. Z.; Blaker, J. J.; Boccaccini, A. R., Biodegradable and bioactive porous polymer/inorganic composite scaffolds for bone tissue engineering. Biomaterials 2006, 27 (18), 3413-3431. DOI: http://dx.doi.org/10.1016/j.biomaterials.2006.01.039.
[47] Rhee, S.-H.; Choi, J.-Y.; Kim, H.-M., Preparation of a bioactive and degradable PCL/silica hybrid through a sol-gel method. Biomaterials 2002, 23 (24), 4915-4921. DOI: http://dx.doi.org/10.1016/S0142-9612(02)00251-X.
[48] Allan, I.; Newman, H.; Wilson, M., Antibacterial activity of particulate Bioglass® against supra- and subgingival bacteria. Biomaterials 2001, 22 (12), 1683-1687. DOI: http://dx.doi.org/10.1016/S0142-9612(00)00330-6.
[49] Hynes, R. O., Integrins: versatility, modulation, and signaling in cell adhesion. Cell 1992, 69 (1), 11-25. DOI: http://dx.doi.org/10.1016/0092-8674(92)90115-S.
[50] Jianhua, W.; Toshio, I.; Naoto, O.; Takayasu, I.; Takashi, M.; Baolin, L.; Masao, Y., Influence of surface wettability on competitive protein adsorption and initial attachment of osteoblasts. Biomedical Materials 2009, 4 (4), 045002.
[51] Brodbeck, W. G.; Shive, M. S.; Colton, E.; Nakayama, Y.; Matsuda, T.; Anderson, J. M., Influence of biomaterial surface

chemistry on the apoptosis of adherent cells. J. Biomed. Mater. Res. 2001, 55 (4), 661-668. DOI: 10.1002/1097-4636(20010615)55:4<661::aid-jbm1061>3.0.co;2-f.

[52] Brodbeck, W. G.; Patel, J.; Voskerician, G.; Christenson, E.; Shive, M. S.; Nakayama, Y.; Matsuda, T.; Ziats, N. P.; Anderson, J. M., Biomaterial adherent macrophage apoptosis is increased by hydrophilic and anionic substrates in vivo. Proc. Natl. Acad. Sci. U. S. A. 2002, 99 (16), 10287-10292. DOI: 10.1073/pnas.162124199.

[53] Olmo, N.; Martı; x; n, A. I.; Salinas, A. J.; Turnay, J.; Vallet, R.; x; Marı; x; Lizarbe, M. A., Bioactive sol–gel glasses with and without a hydroxycarbonate apatite layer as substrates for osteoblast cell adhesion and proliferation. Biomaterials 2003, 24 (20), 3383-3393. DOI: https://doi.org/10.1016/S0142-9612(03)00200-X.

[54] Schmidt-Bleek, K.; Schell, H.; Schulz, N.; Hoff, P.; Perka, C.; Buttgereit, F.; Volk, H.-D.; Lienau, J.; Duda, G. N., Inflammatory phase of bone healing initiates the regenerative healing cascade. Cell Tissue Res. 2012, 347 (3), 567-573. DOI: 10.1007/s00441-011-1205-7.

[55] Lai, W.; Garino, J.; Ducheyne, P., Silicon excretion from bioactive glass implanted in rabbit bone. Biomaterials 2002, 23 (1), 213-217. DOI: http://dx.doi.org/10.1016/S0142-9612(01)00097-7.

Supplementary materials

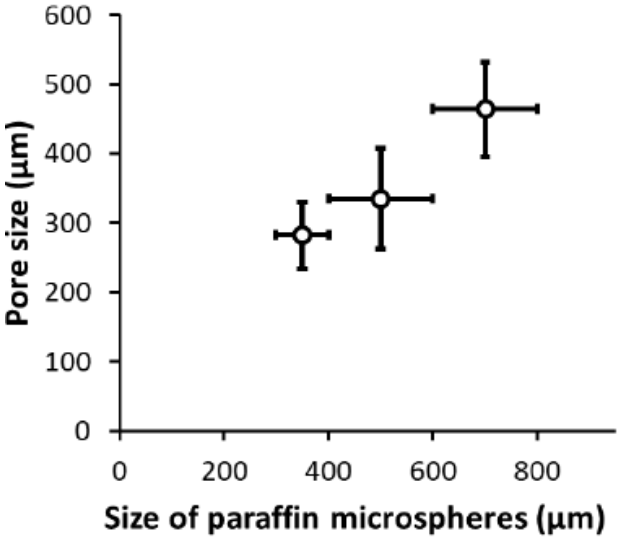

ESI 1: Variation of pore size as a function of the porogen size.

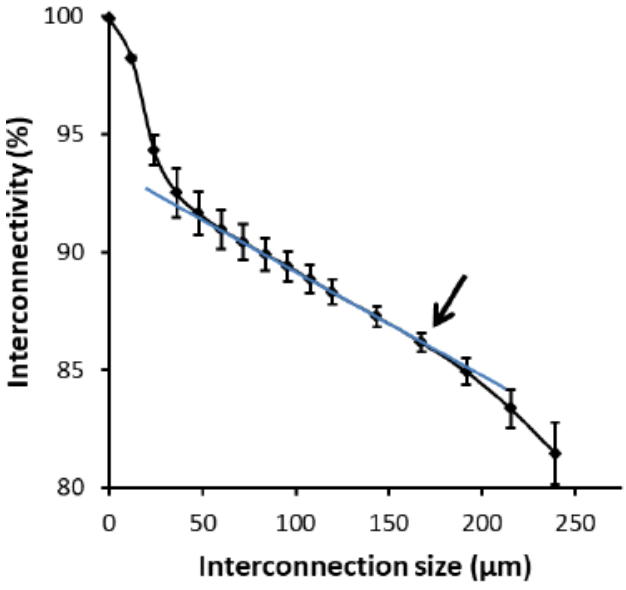

ESI 2: Interconnectivity analysis of BG-PCL hybrid scaffolds. The interconnectivity starts reducing at a faster rate from 175-190 µm onwards, suggesting that the mean interconnection size is around this area. The initial reduction is due to micropores in the scaffold walls.

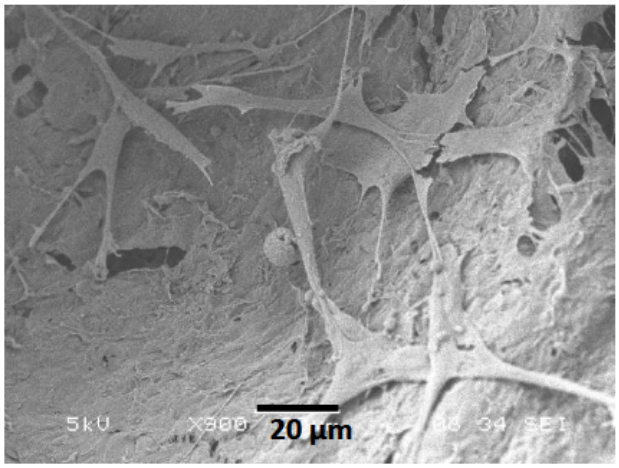

ESI 3: SEM image of primary osteoblasts cultured in BG-PCL hybrid scaffolds.